Regulation of deep and shallow hole/electron trap states and charge conducting behaviors of dielectric tribo-materials for maximizing retained charges

Jian Wang,[a‡] Shuyan Xu,[a‡] Gui Li,[a] Huiyuan Wu,[a] Kaixian Li,[a] Ai Chen,[a] Qionghua Zhao,[a] Shaoke Fu,[a] Chuncai Shan,[a] Yi Xi[a] and Chenguo Hu*[a]*

[a] Department of Applied Physics, Chongqing Key Laboratory of Soft Condensed Matter Physics and Smart Materials, Chongqing University, Chongqing 400044, P.R. China

‡ These authors contributed equally to this work.

Email: yxi6@cqu.edu.cn (Y Xi), hucg@cqu.edu.cn (C Hu)

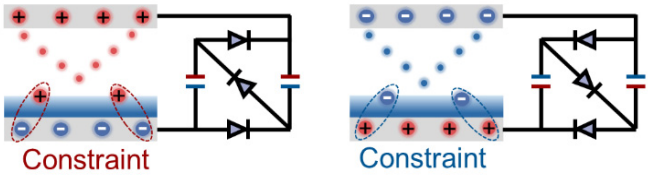

Fig. S1: The binding effect of injected charge on excitation output.

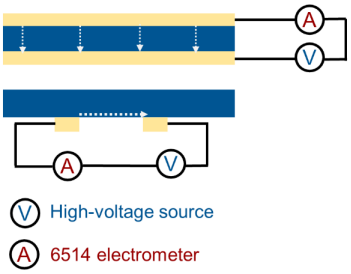

Fig. S2: Test diagram of charge leakage current and surface conduction current.

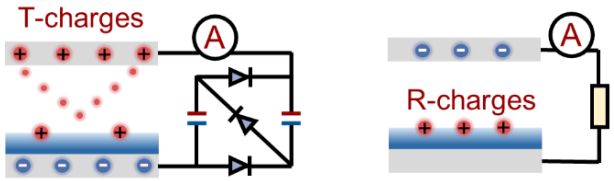

Fig. S3: Test protocol for T-charges and R-charges.

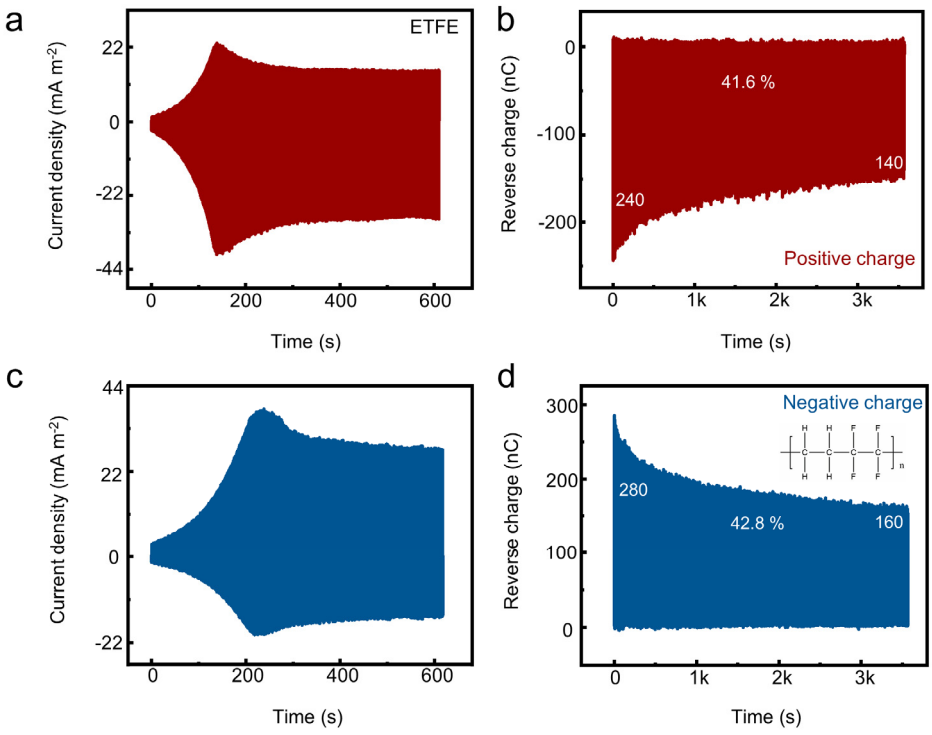

Fig. S4: The output characteristics of UH-CSI-TENG with ETFE as triboelectric material. a) Dynamic current density output with positive charge injection, b) Charge dissipation of the injected positive charge, c) Dynamic current density output with negative charge injection, and d) Charge dissipation of the injected negative charge, using ETFE film as the dielectric layer.

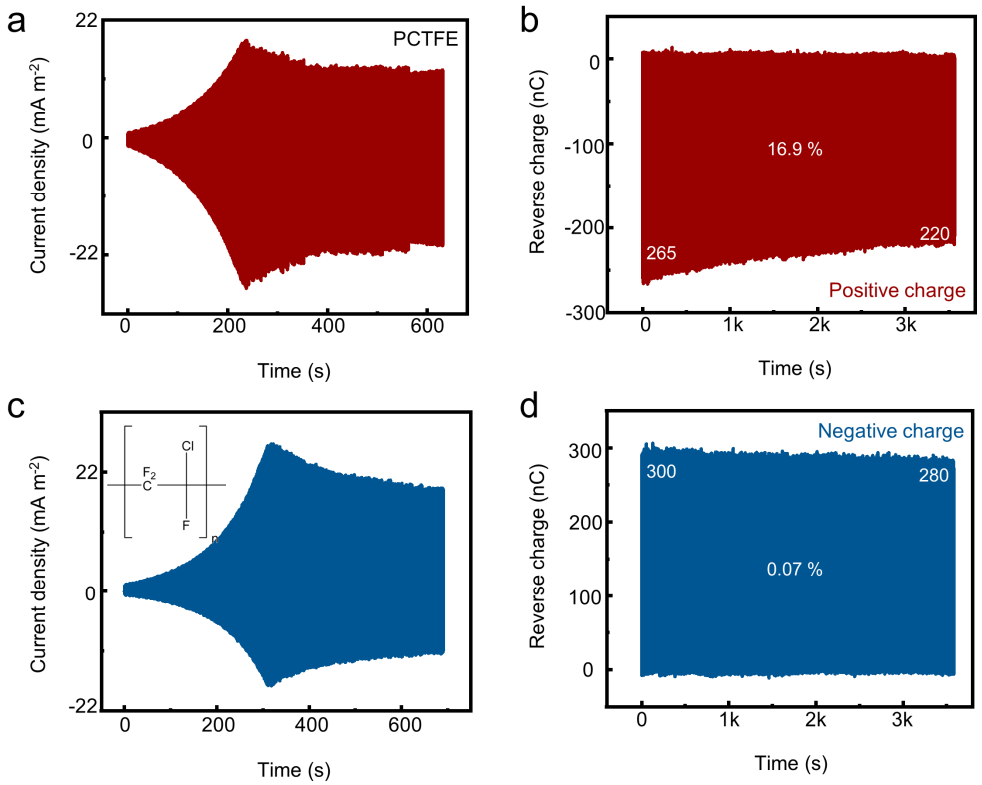

Fig. S5: The output characteristics of UH-CSI-TENG with PCTFE as triboelectric material. a) Dynamic current density output with positive charge injection, b) Charge dissipation of the injected positive charge, c) Dynamic current density output with negative charge injection, and d) Charge dissipation of the injected negative charge, using PCTFE film as the dielectric layer.

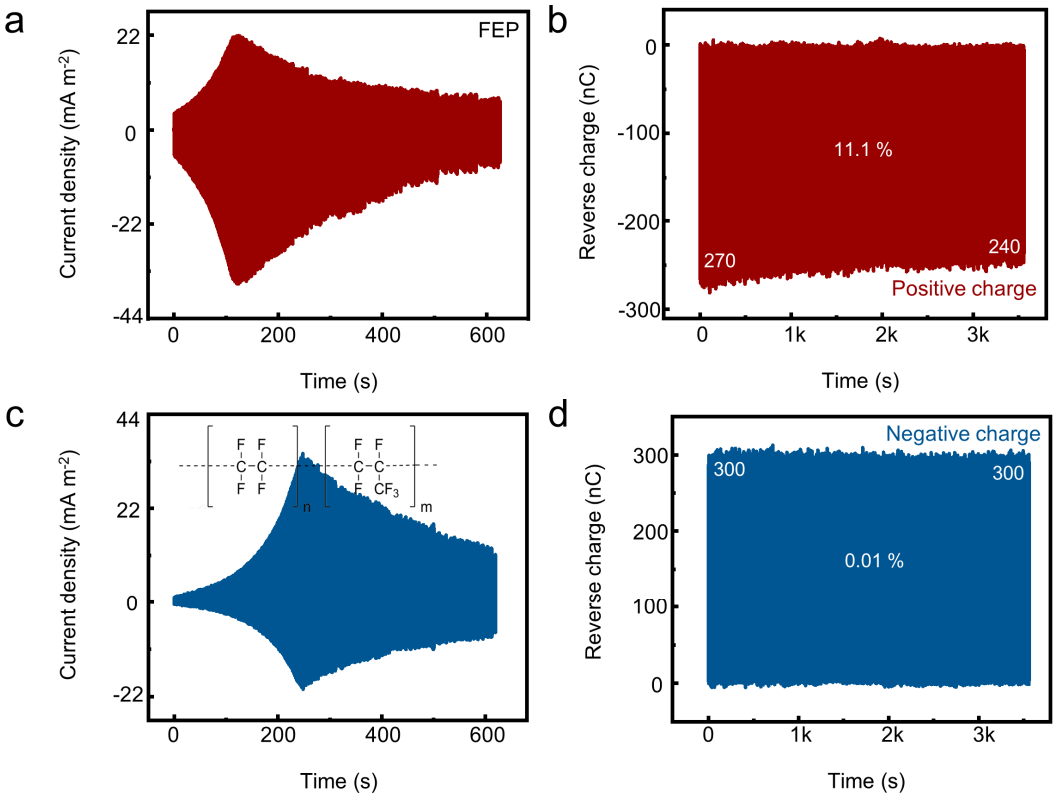

Fig. S6: The output characteristics of UH-CSI-TENG with FEP as triboelectric material. a) Dynamic current density output with positive charge injection, b) Charge dissipation of the injected positive charge, c) Dynamic current density output with negative charge injection, and d) Charge dissipation of the injected negative charge, using FEP film as the dielectric layer.

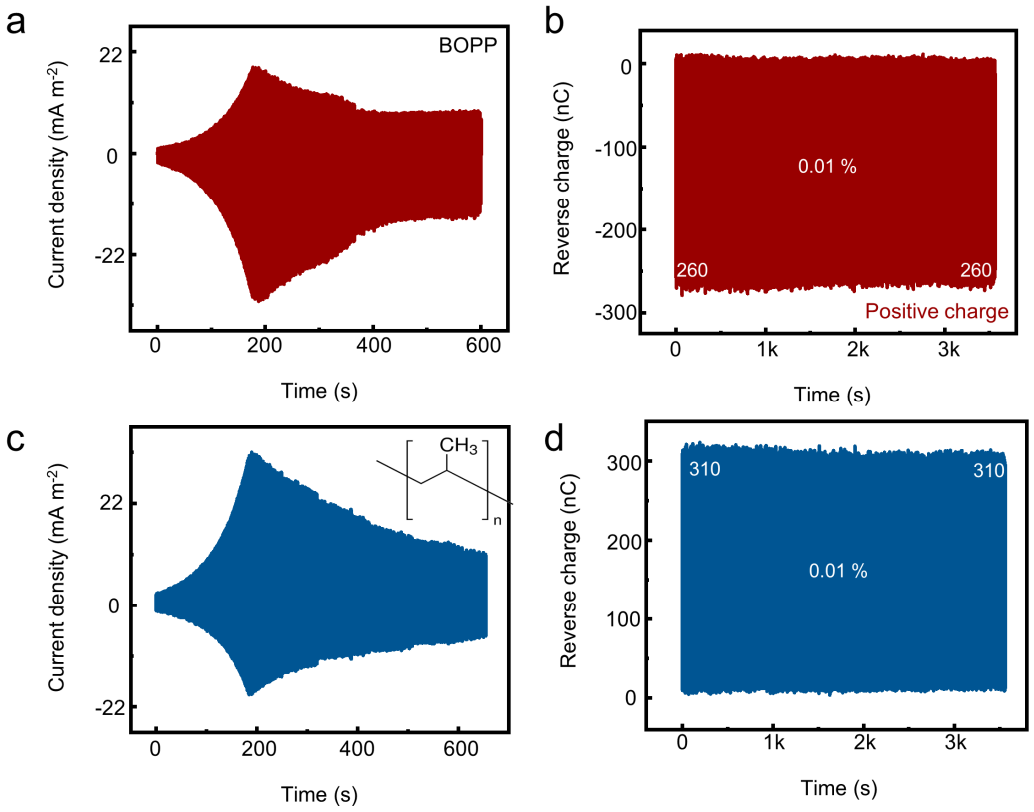

Fig. S7: The output characteristics of UH-CSI-TENG with BOPP as triboelectric material. a) Dynamic current density output with positive charge injection, b) Charge dissipation of the injected positive charge, c) Dynamic current density output with negative charge injection, and d) Charge dissipation of the injected negative charge, using BOPP film as the dielectric layer.

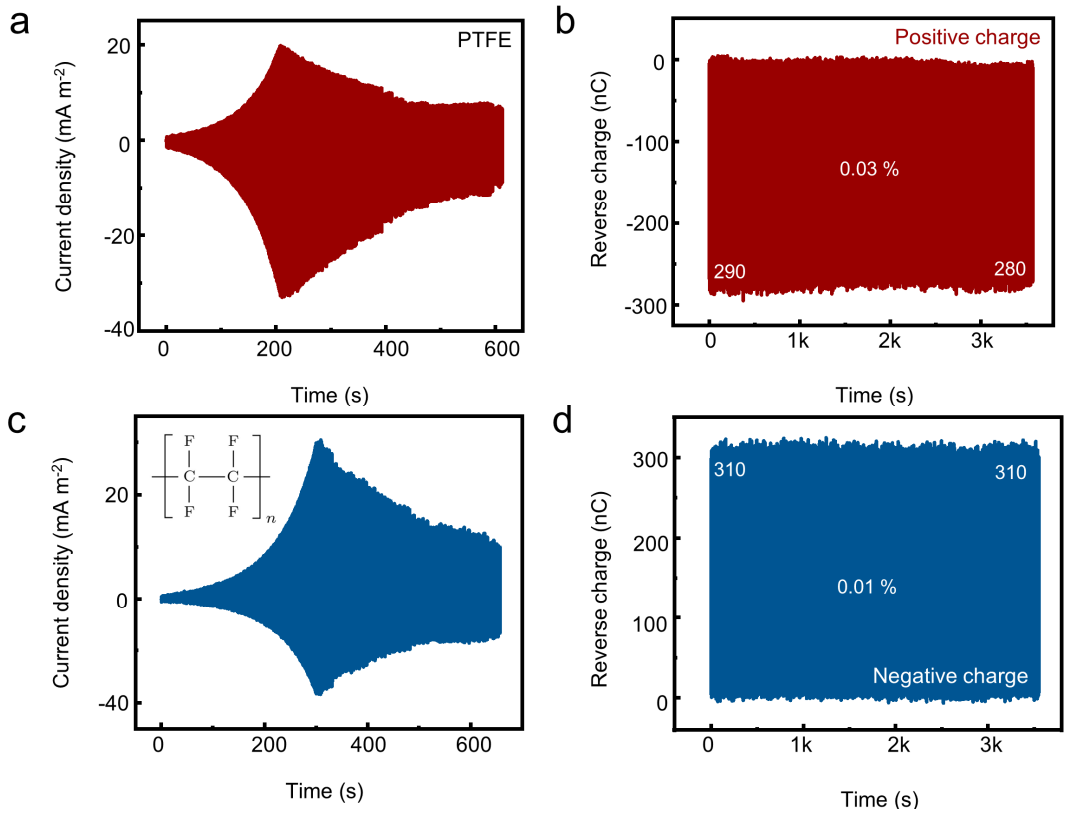

Fig. S8: The output characteristics of UH-CSI-TENG with PTFE as triboelectric material. a) Dynamic current density output with positive charge injection, b) Charge dissipation of the injected positive charge, c) Dynamic current density output with negative charge injection, and d) Charge dissipation of the injected negative charge, using PTFE film as the dielectric layer.

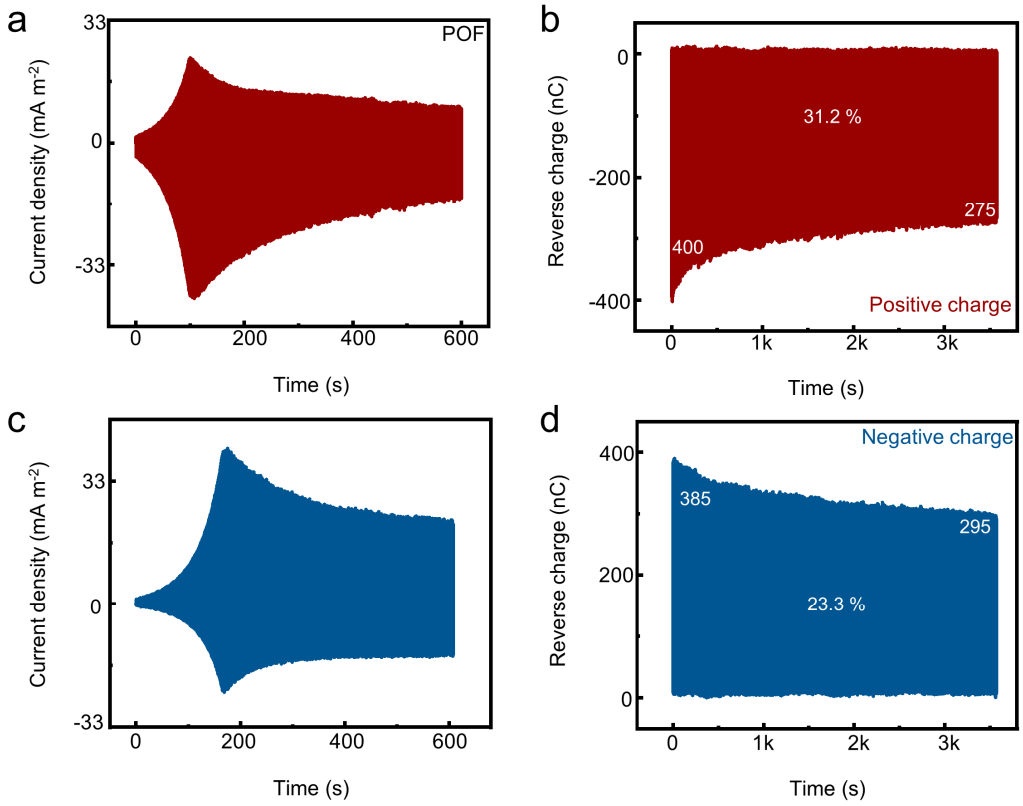

Fig. S9: The output characteristics of UH-CSI-TENG with POF as triboelectric material. a) Dynamic current density output with positive charge injection, b) Charge dissipation of the injected positive charge, c) Dynamic current density output with negative charge injection, and d) Charge dissipation of the injected negative charge, using POF film as the dielectric layer.

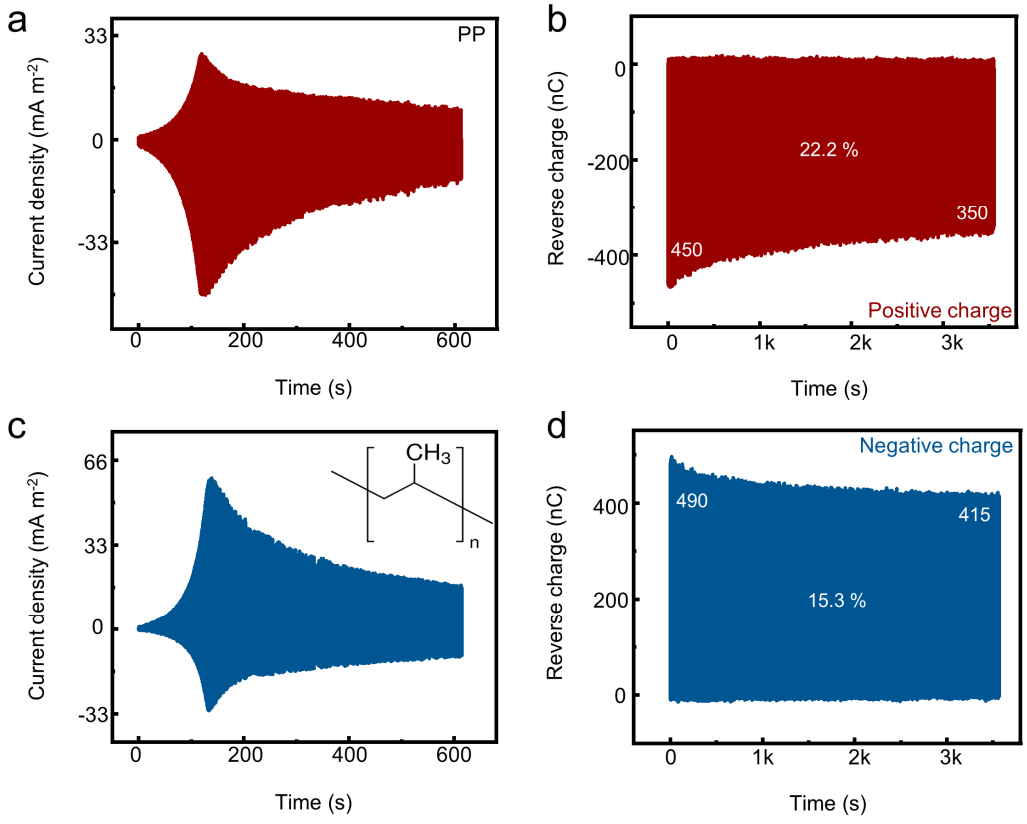

Fig. S10: The output characteristics of UH-CSI-TENG with PP as triboelectric material. a) Dynamic current density output with positive charge injection, b) Charge dissipation of the injected positive charge, c) Dynamic current density output with negative charge injection, and d) Charge dissipation of the injected negative charge, using PP film as the dielectric layer.

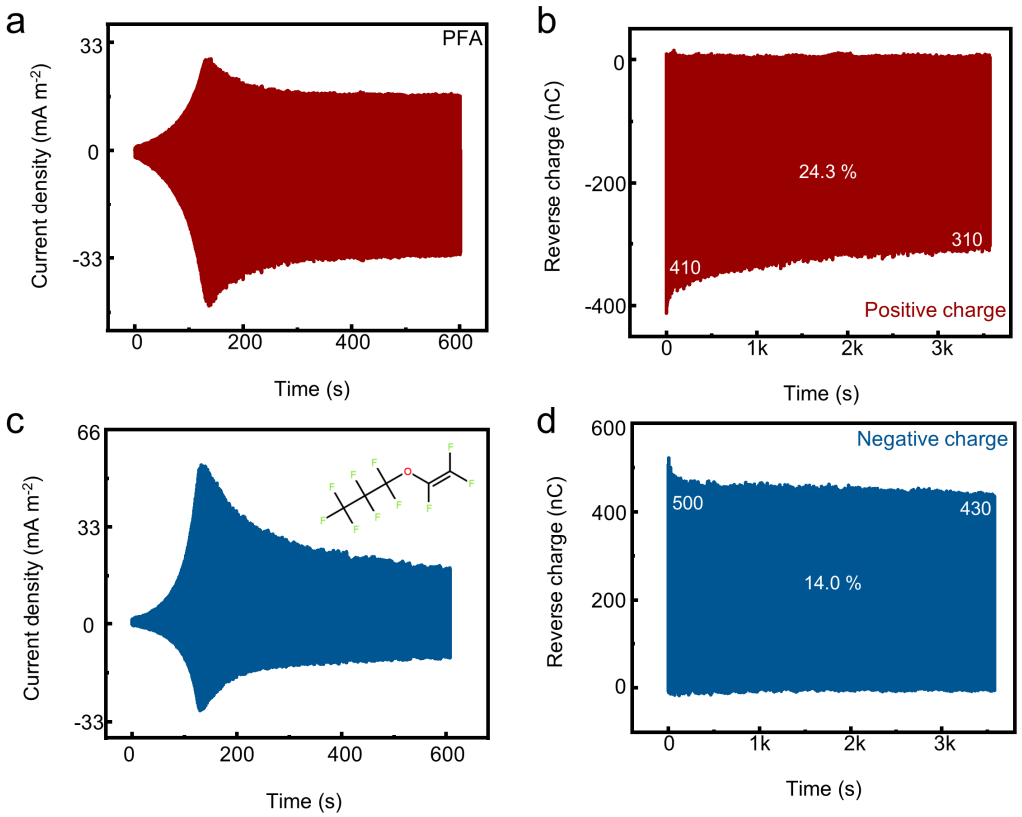

Fig. S11: The output characteristics of UH-CSI-TENG with PFA as triboelectric material. a) Dynamic current density output with positive charge injection, b) Charge dissipation of the injected positive charge, c) Dynamic current density output with negative charge injection, and d) Charge dissipation of the injected negative charge, using PFA film as the dielectric layer.

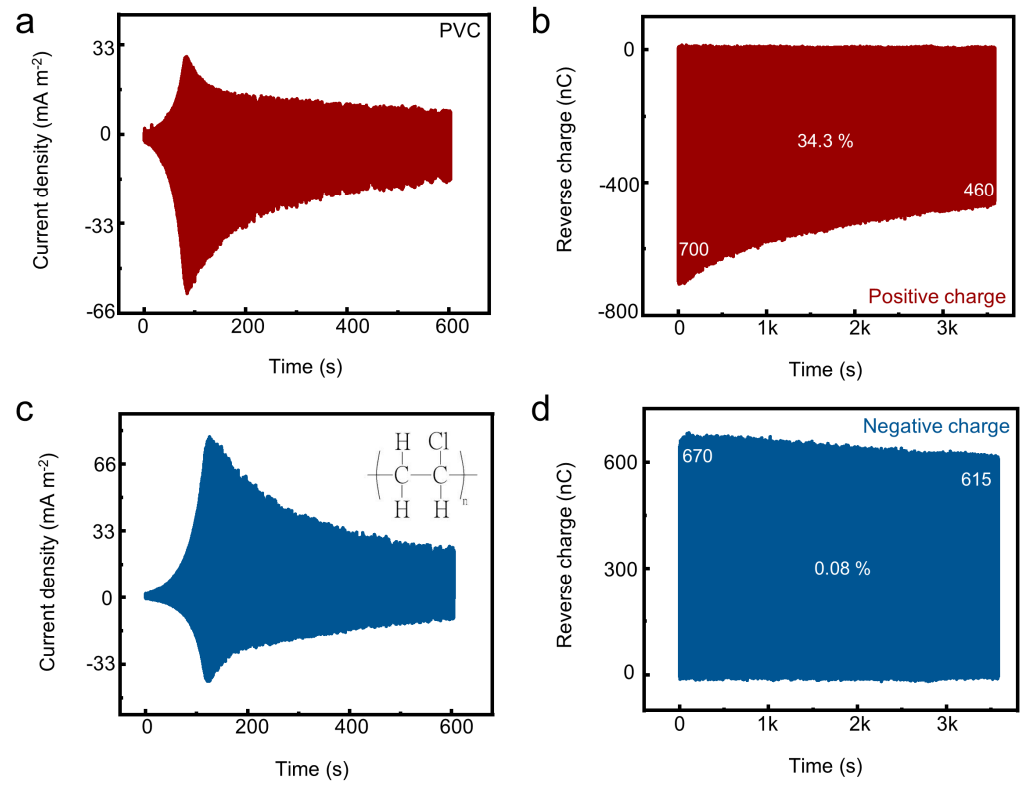

Fig. S12: The output characteristics of UH-CSI-TENG with PVC as triboelectric material. a) Dynamic current density output with positive charge injection, b) Charge dissipation of the injected positive charge, c) Dynamic current density output with negative charge injection, and d) Charge dissipation of the injected negative charge, using PVC film as the dielectric layer.

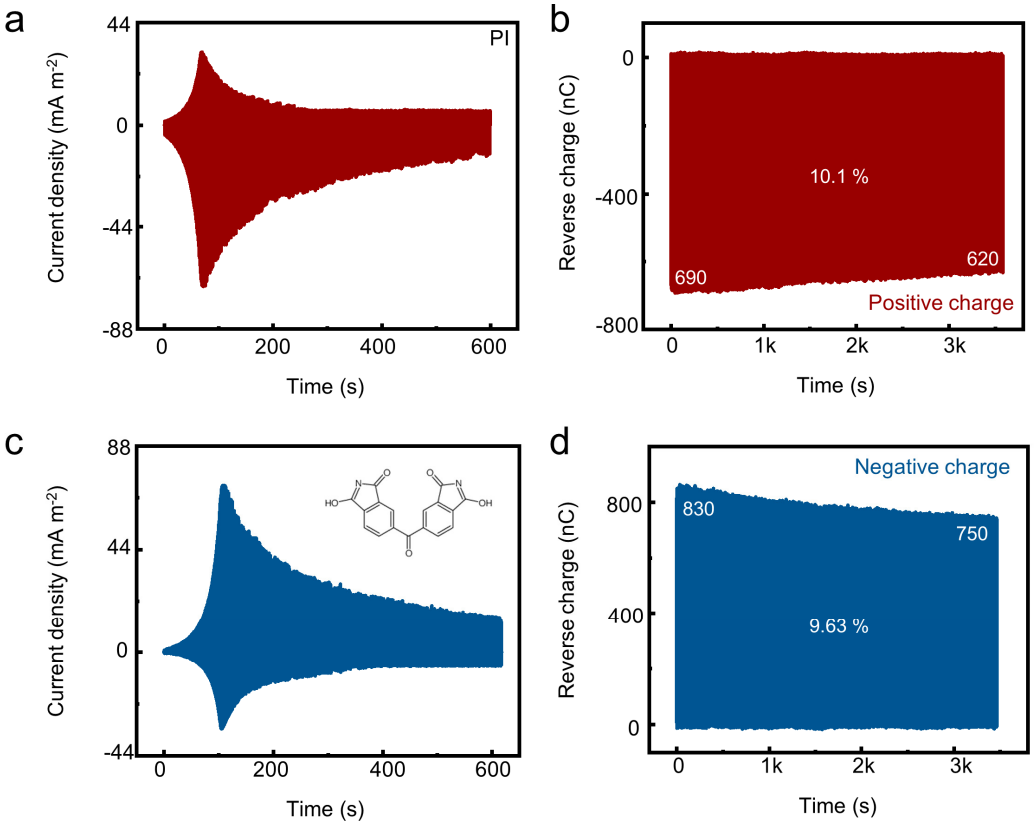

Fig. S13: The output characteristics of UH-CSI-TENG with PI as triboelectric material. a) Dynamic current density output with positive charge injection, b) Charge dissipation of the injected positive charge, c) Dynamic current density output with negative charge injection, and d) Charge dissipation of the injected negative charge, using PI film as the dielectric layer.

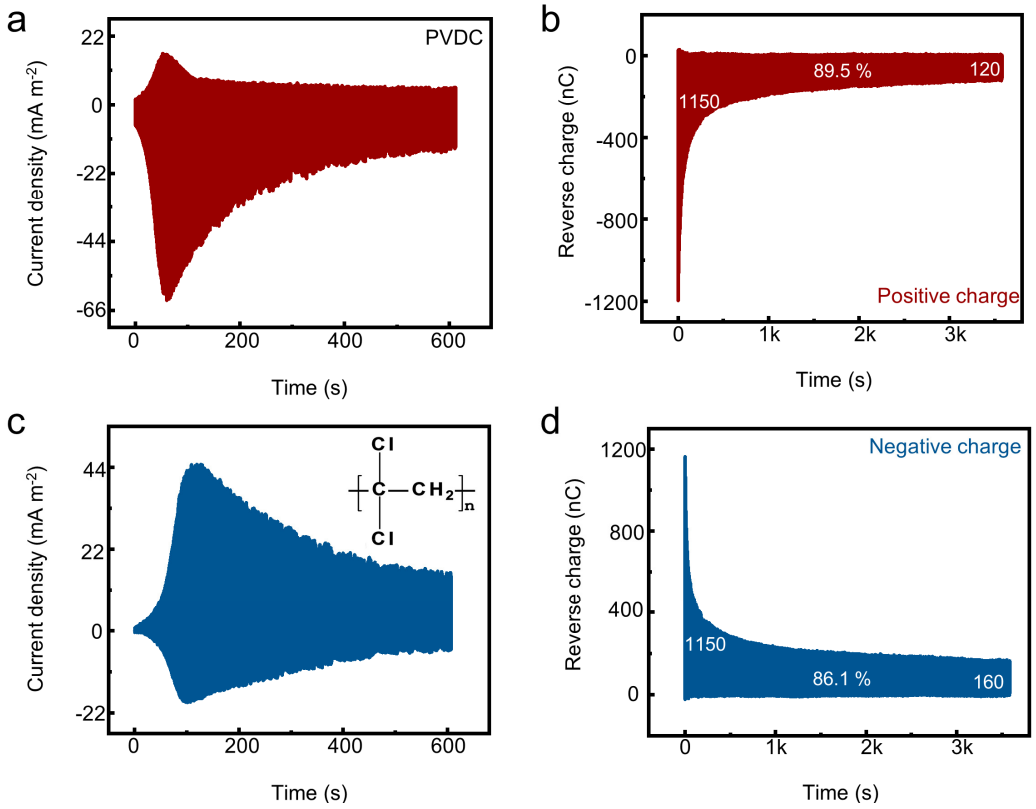

Fig. S14: The output characteristics of UH-CSI-TENG with PVDC as triboelectric material. a) Dynamic current density output with positive charge injection, b) Charge dissipation of the injected positive charge, c) Dynamic current density output with negative charge injection, and d) Charge dissipation of the injected negative charge, using PVDC film as the dielectric layer.

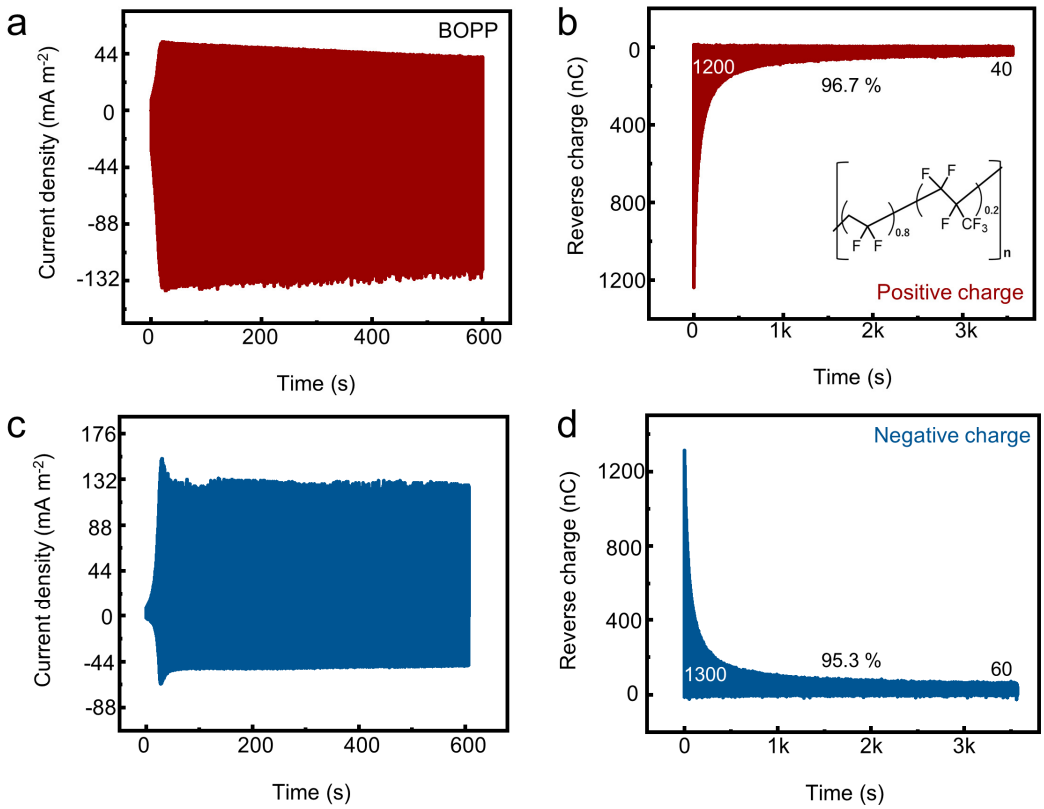

Fig. S15: The output characteristics of UH-CSI-TENG with BOPP as triboelectric material. a) Dynamic current density output with positive charge injection, b) Charge dissipation of the injected positive charge, c) Dynamic current density output with negative charge injection, and d) Charge dissipation of the injected negative charge, using BOPP film as the dielectric layer.

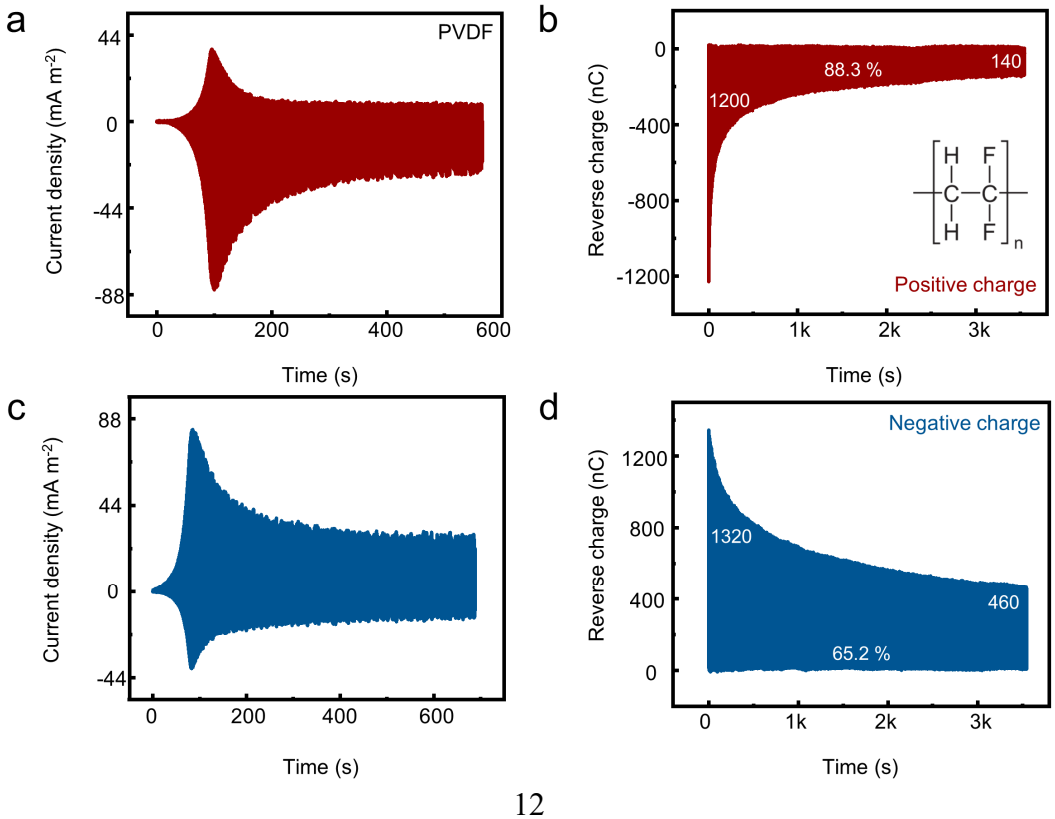

Fig. S16: The output characteristics of UH-CSI-TENG with PVDF as triboelectric material. a) Dynamic current density output with positive charge injection, b) Charge dissipation of the injected positive charge, c) Dynamic current density output with negative charge injection, and d) Charge dissipation of the injected negative charge, using PVDF film as the dielectric layer.

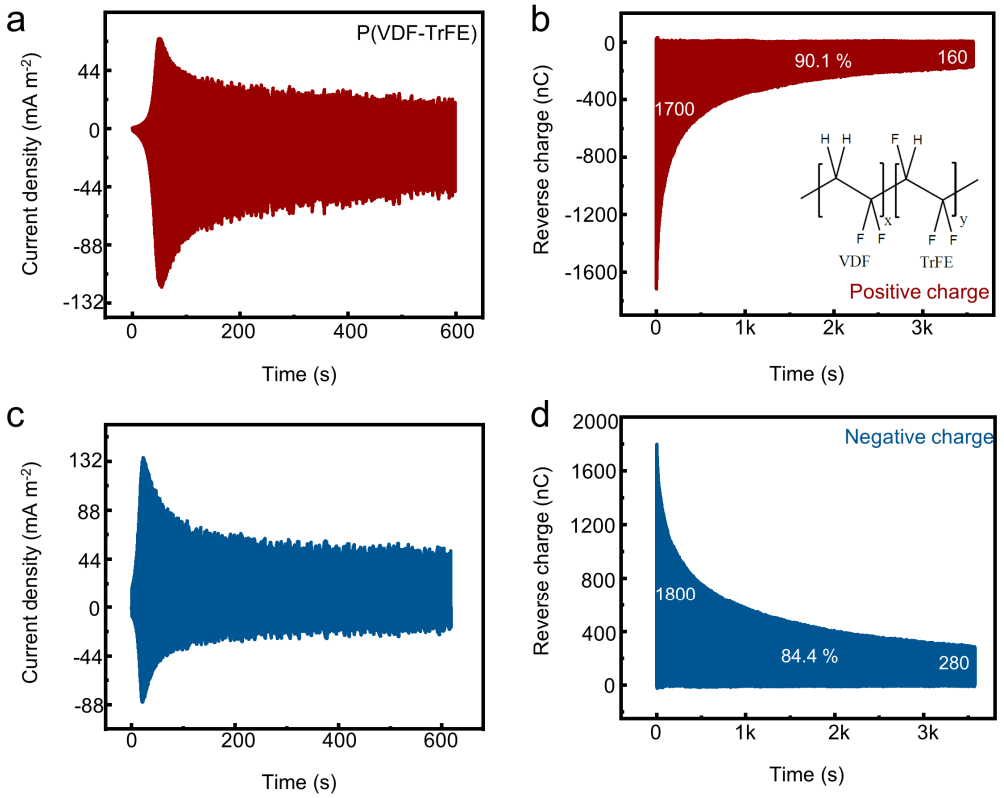

Fig. S17: The output characteristics of UH-CSI-TENG with P(VDF-TrFE) as triboelectric material. a) Dynamic current density output with positive charge injection, b) Charge dissipation of the injected positive charge, c) Dynamic current density output with negative charge injection, and d) Charge dissipation of the injected negative charge, using P(VDF-TrFE) film as the dielectric layer.

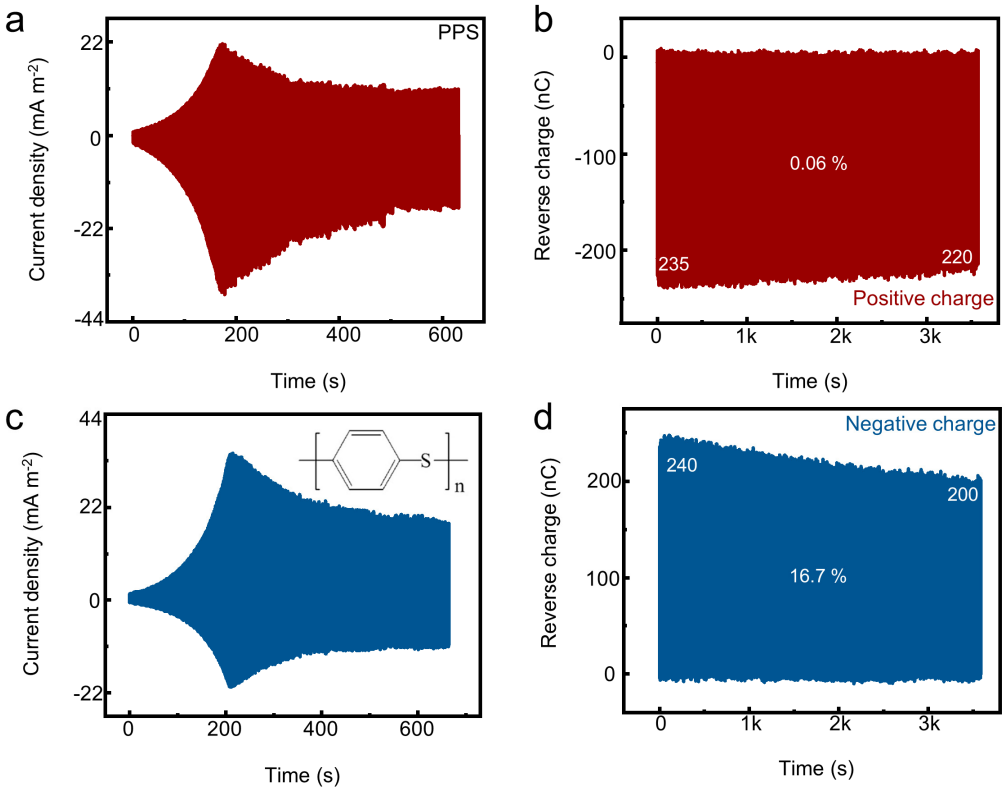

Fig. S18: The output characteristics of UH-CSI-TENG with PPS as triboelectric material. a) Dynamic current density output with positive charge injection, b) Charge dissipation of the injected positive charge, c) Dynamic current density output with negative charge injection, and d) Charge dissipation of the injected negative charge, using PPS film as the dielectric layer.

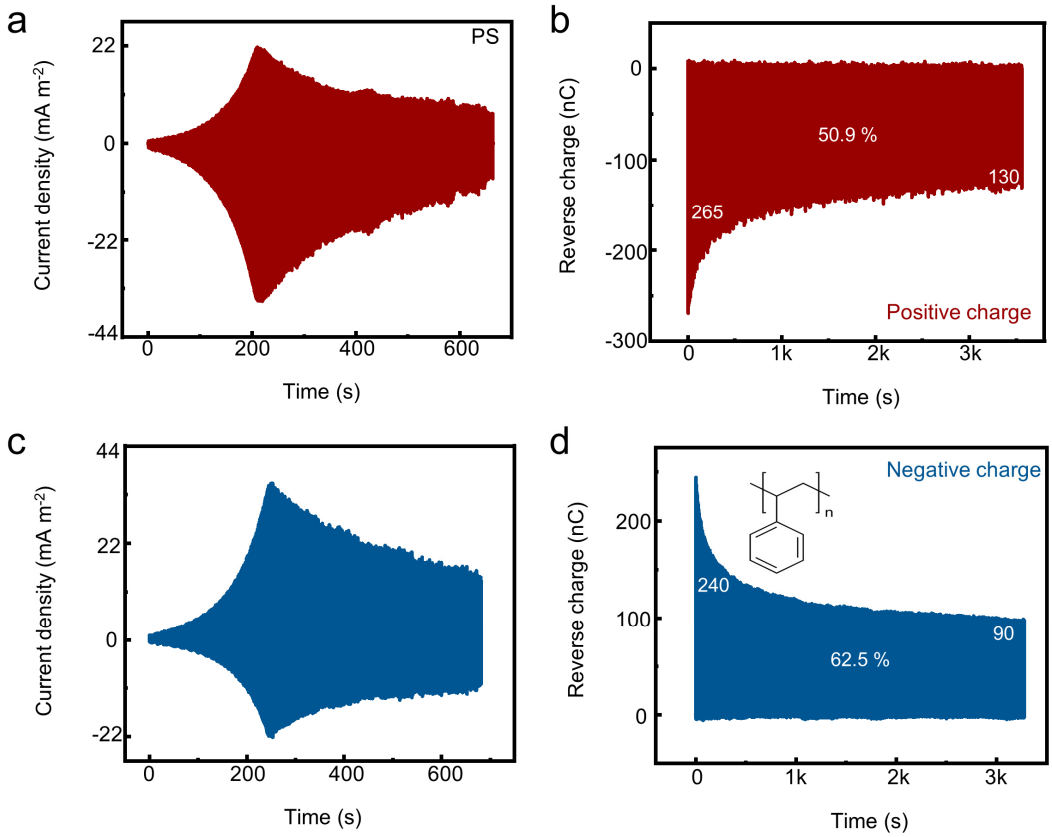

Fig. S19: The output characteristics of UH-CSI-TENG with PS as triboelectric material. a) Dynamic current density output with positive charge injection, b) Charge dissipation of the injected positive charge, c) Dynamic current density output with negative charge injection, and d) Charge dissipation of the injected negative charge, using PS film as the dielectric layer.

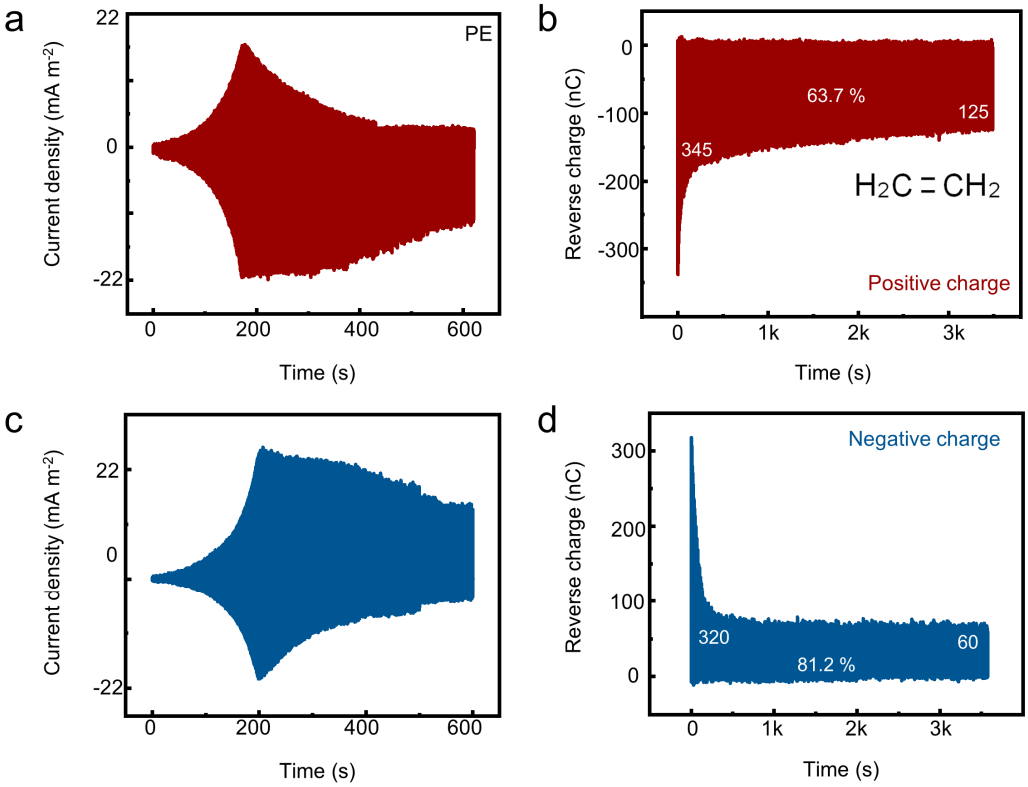

Fig. S20: The output characteristics of UH-CSI-TENG with PE as triboelectric material. a) Dynamic current density output with positive charge injection, b) Charge dissipation of the injected positive charge, c) Dynamic current density output with negative charge injection, and d) Charge dissipation of the injected negative charge, using PE film as the dielectric layer.

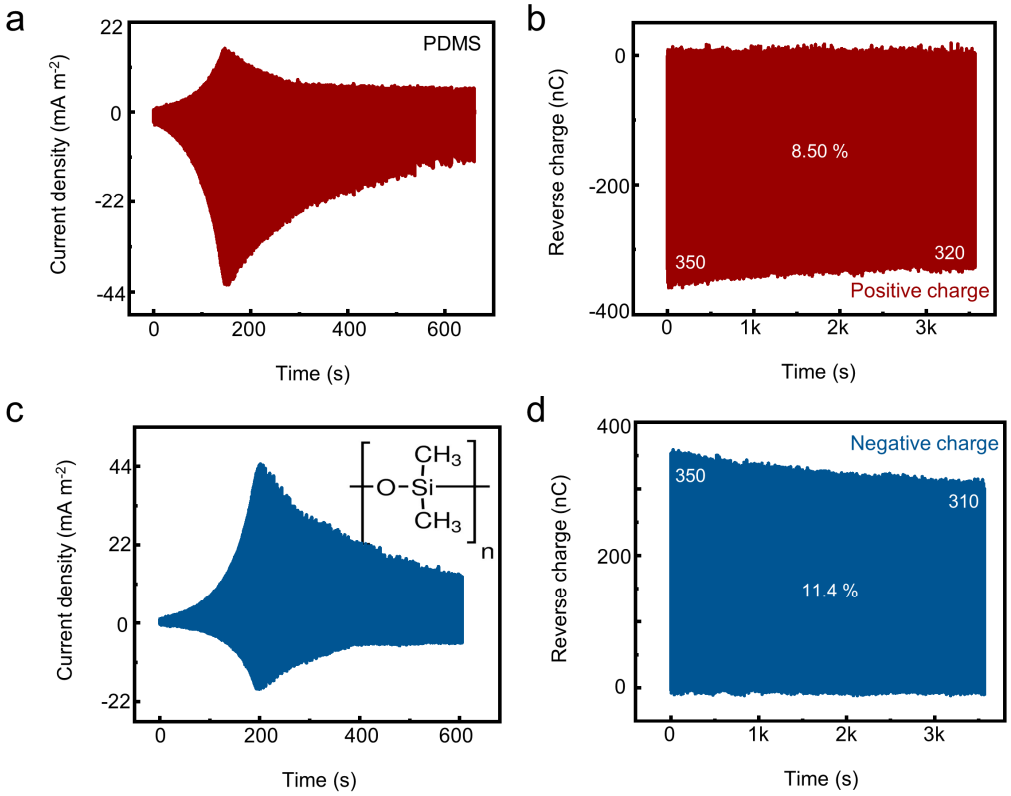

Fig. S21: The output characteristics of UH-CSI-TENG with PDMS as triboelectric material. a) Dynamic current density output with positive charge injection, b) Charge dissipation of the injected positive charge, c) Dynamic current density output with negative charge injection, and d) Charge dissipation of the injected negative charge, using PDMS film as the dielectric layer.

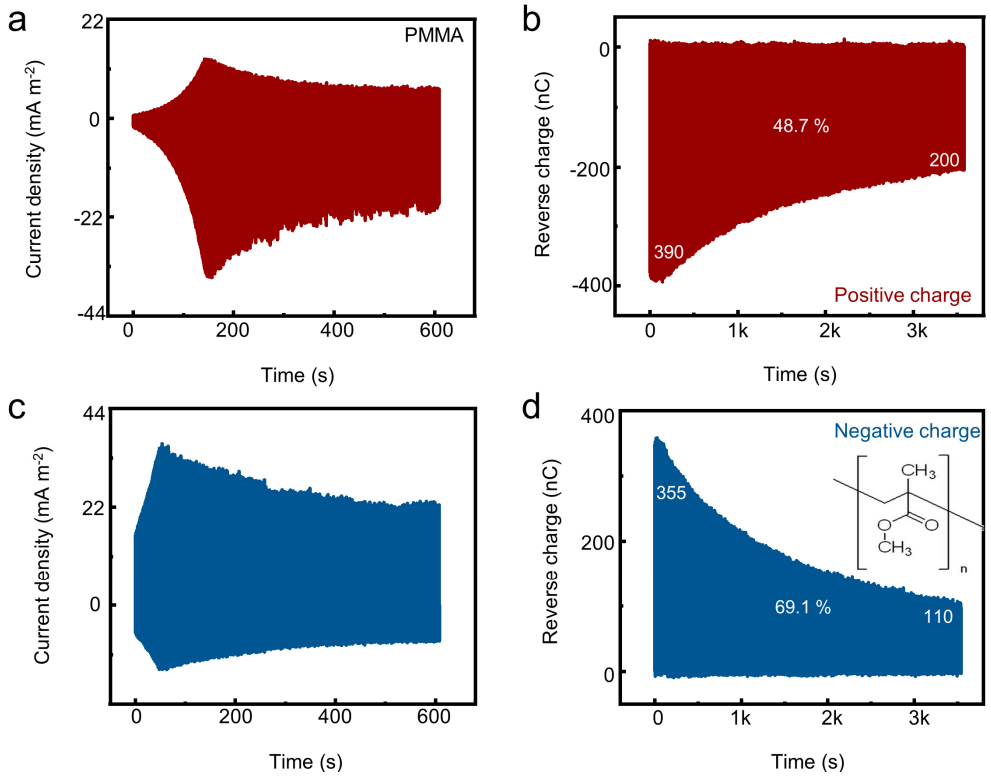

Fig. S22: The output characteristics of UH-CSI-TENG with PMMA as triboelectric material. a) Dynamic current density output with positive charge injection, b) Charge dissipation of the injected positive charge, c) Dynamic current density output with negative charge injection, and d) Charge dissipation of the injected negative charge, using PMMA film as the dielectric layer.

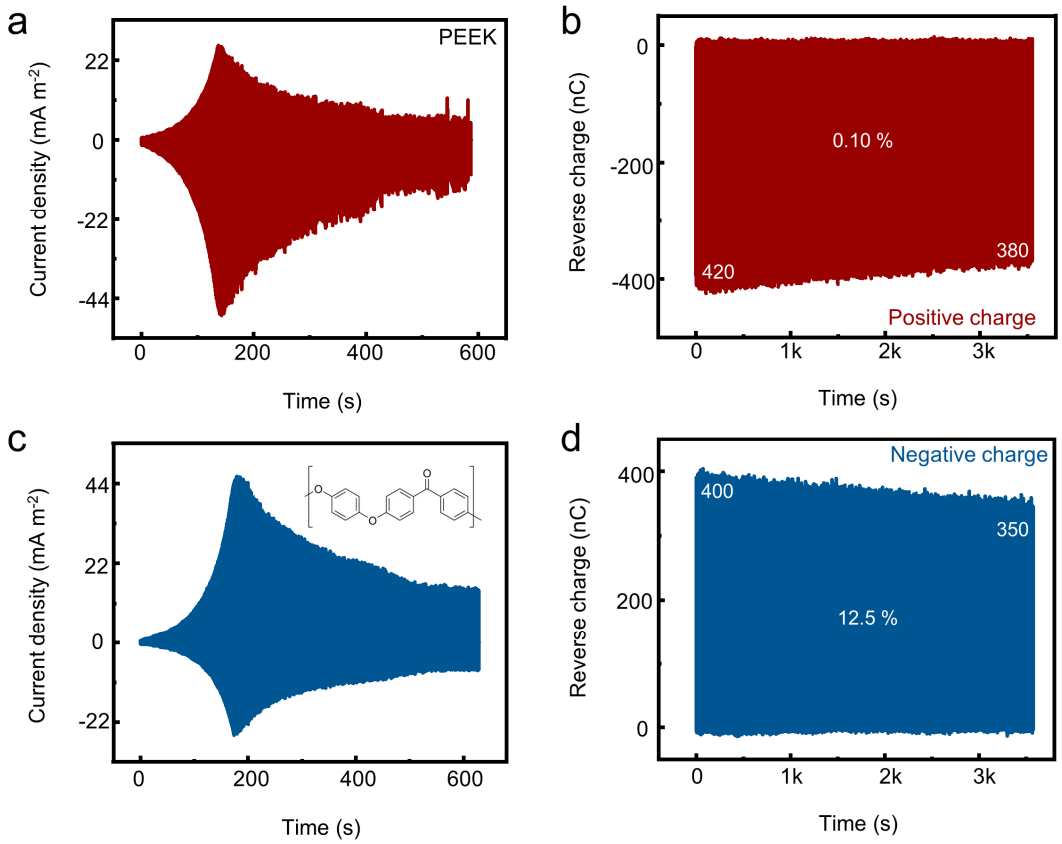

Fig. S23: The output characteristics of UH-CSI-TENG with PEEK as triboelectric material. a) Dynamic current density output with positive charge injection, b) Charge dissipation of the injected positive charge, c) Dynamic current density output with negative charge injection, and d) Charge dissipation of the injected negative charge, using PEEK film as the dielectric layer.

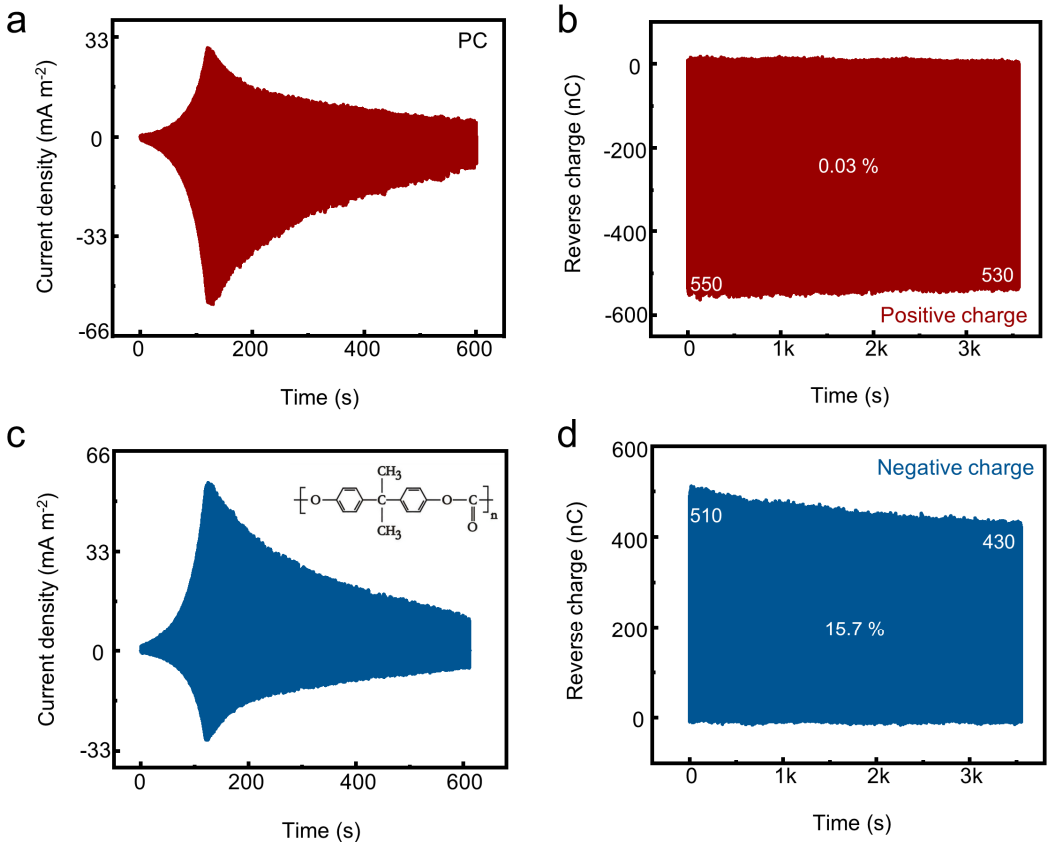

Fig. S24: The output characteristics of UH-CSI-TENG with PC as triboelectric material. a) Dynamic current density output with positive charge injection, b) Charge dissipation of the injected positive charge, c) Dynamic current density output with negative charge injection, and d) Charge dissipation of the injected negative charge, using PC film as the dielectric layer.

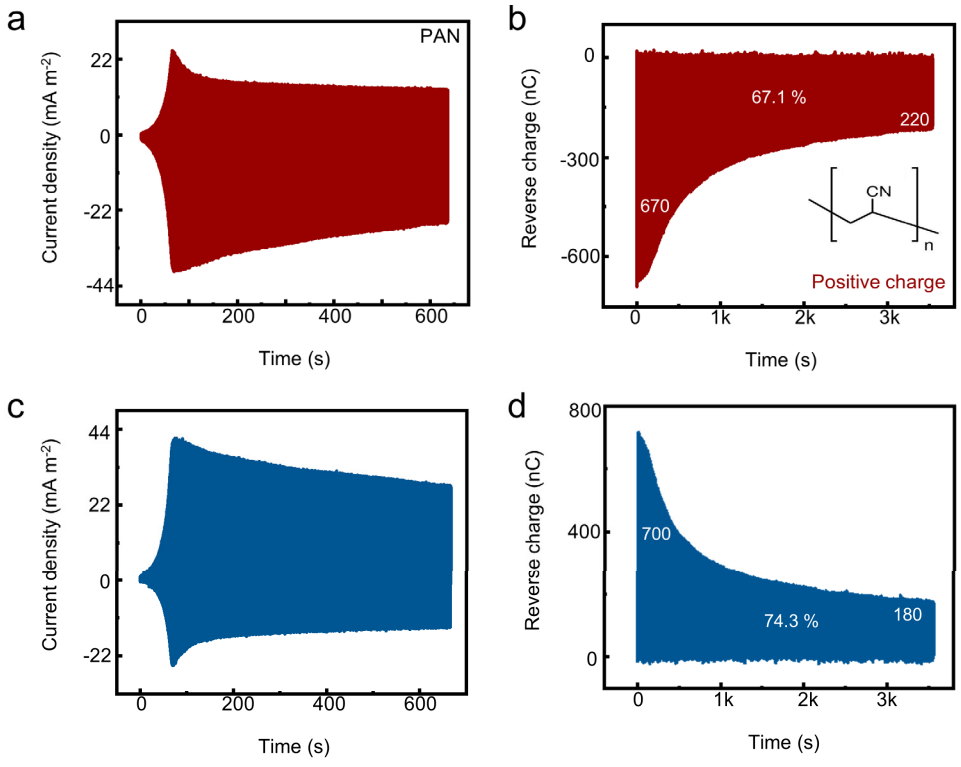

Fig. S25: The output characteristics of UH-CSI-TENG with PAN as triboelectric material. a) Dynamic current density output with positive charge injection, b) Charge dissipation of the injected positive charge, c) Dynamic current density output with negative charge injection, and d) Charge dissipation of the injected negative charge, using PAN film as the dielectric layer.

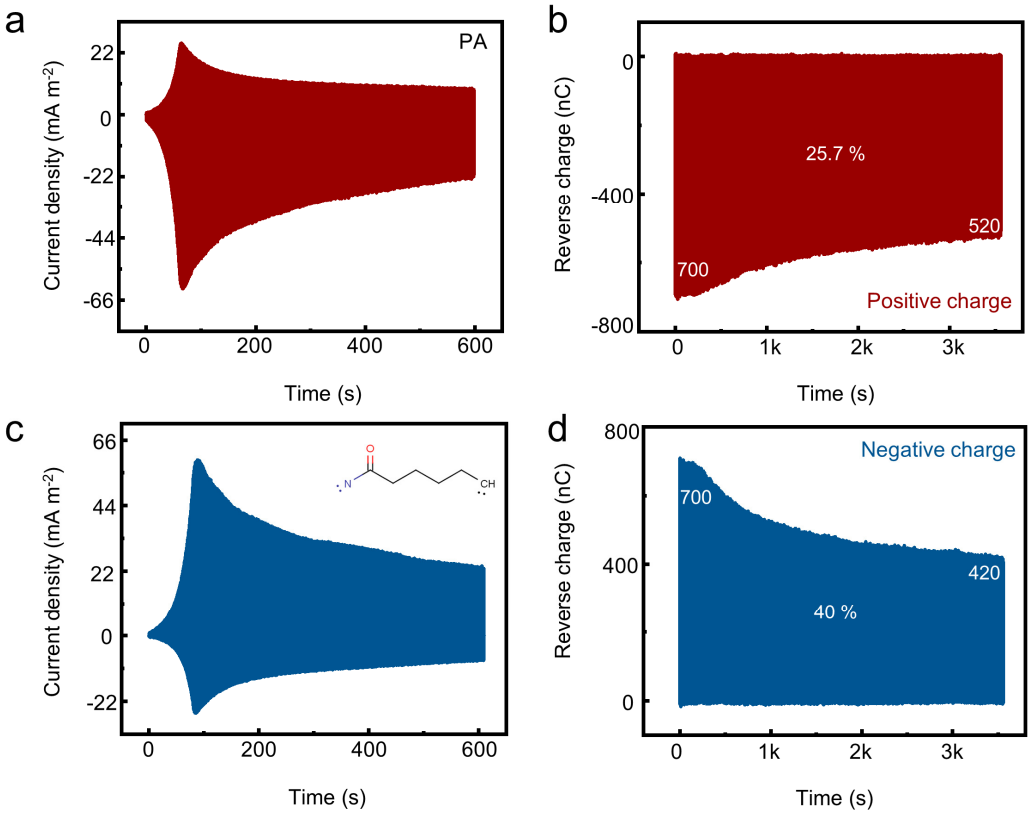

Fig. S26: The output characteristics of UH-CSI-TENG with PA as triboelectric material. a) Dynamic current density output with positive charge injection, b) Charge dissipation of the injected positive charge, c) Dynamic current density output with negative charge injection, and d) Charge dissipation of the injected negative charge, using PA film as the dielectric layer.

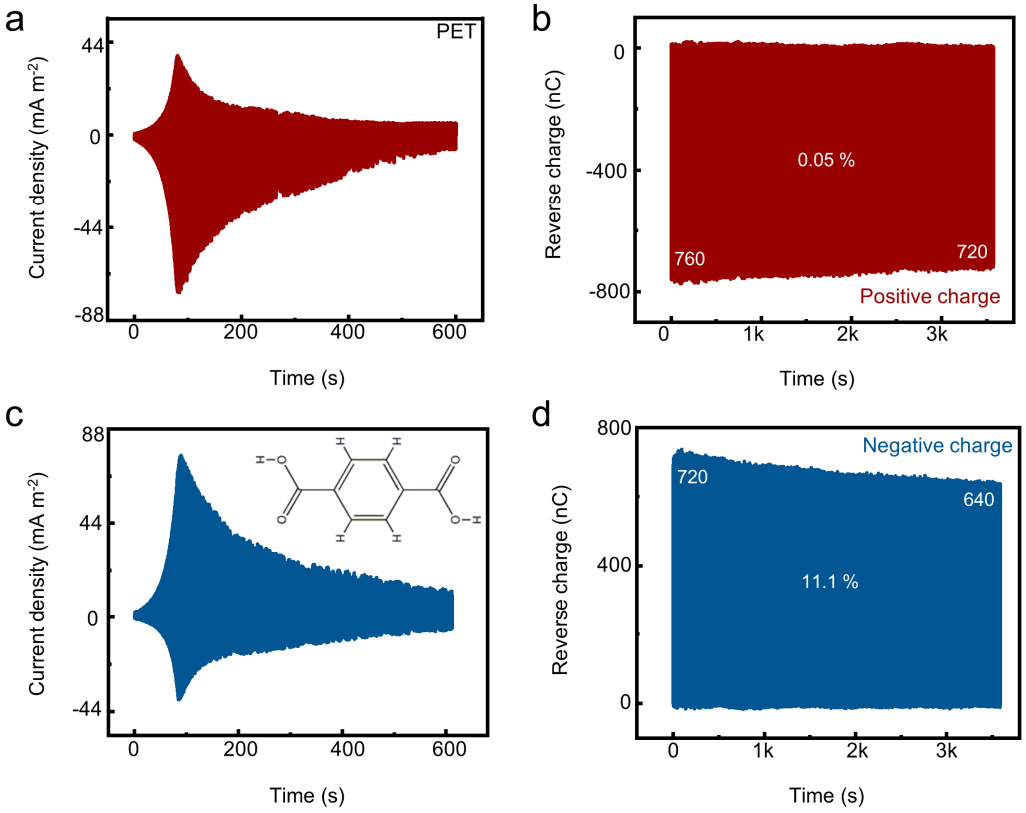

Fig. S27: The output characteristics of UH-CSI-TENG with PET as triboelectric material. a) Dynamic current density output with positive charge injection, b) Charge dissipation of the injected positive charge, c) Dynamic current density output with negative charge injection, and d) Charge dissipation of the injected negative charge, using PET film as the dielectric layer.

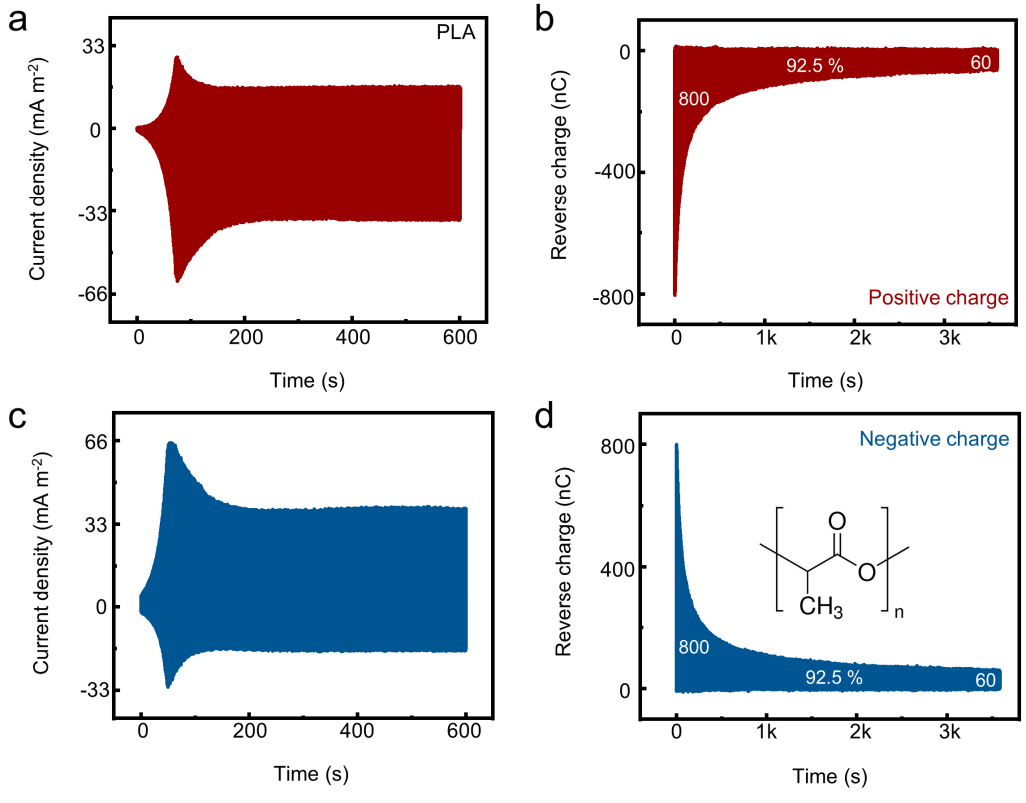

Fig. S28: The output characteristics of UH-CSI-TENG with PLA as triboelectric material. a) Dynamic current density output with positive charge injection, b) Charge dissipation of the injected positive charge, c) Dynamic current density output with negative charge injection, and d) Charge dissipation of the injected negative charge, using PLA film as the dielectric layer.

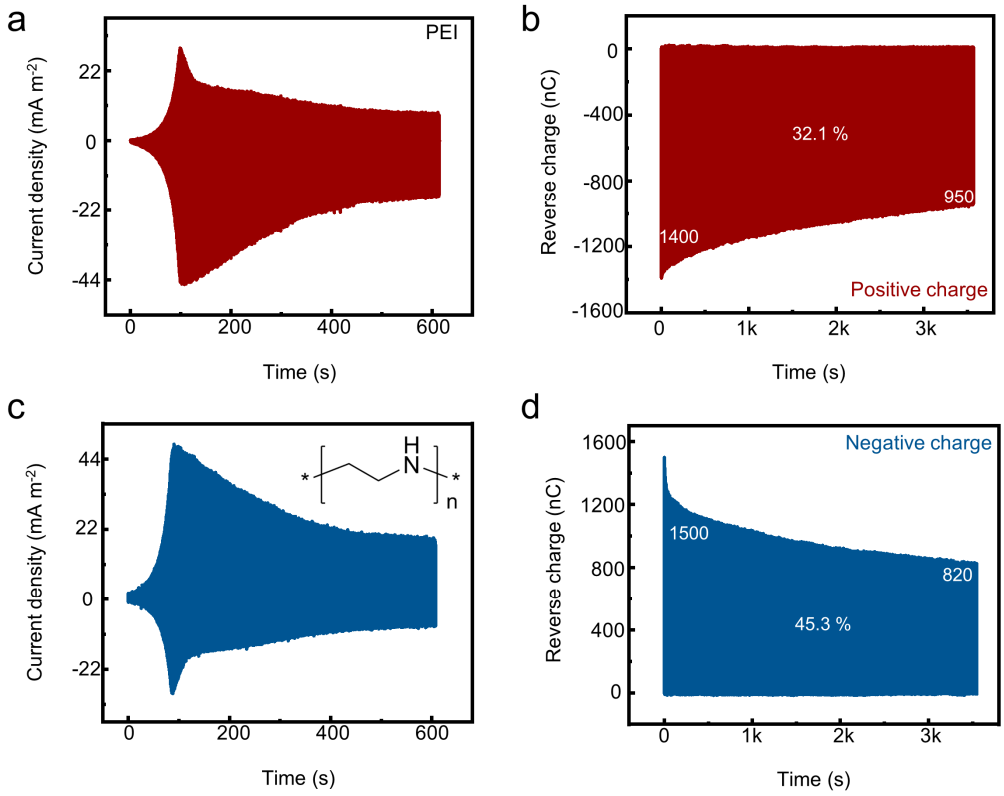

Fig. S29: The output characteristics of UH-CSI-TENG with PEI as triboelectric material. a) Dynamic current density output with positive charge injection, b) Charge dissipation of the injected positive charge, c) Dynamic current density output with negative charge injection, and d) Charge dissipation of the injected negative charge, using PEI film as the dielectric layer.

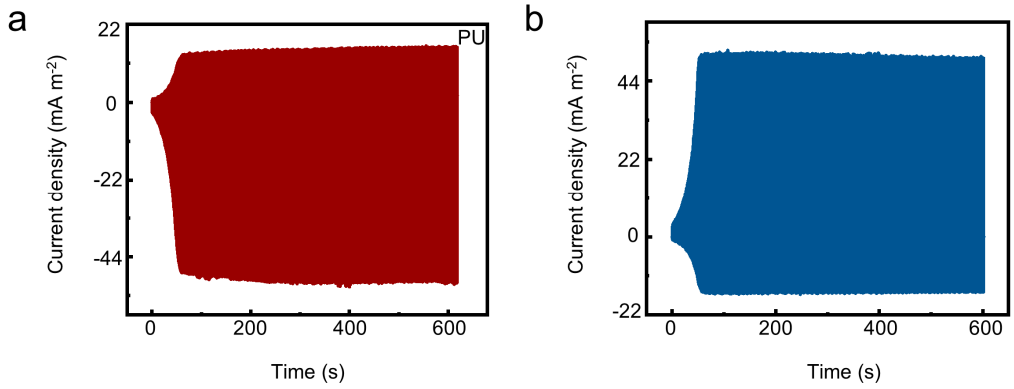

Fig. S30: The output characteristics of UH-CSI-TENG with PU as triboelectric material. a) Dynamic current density output with positive charge injection, and b) Dynamic current density output with negative charge injection, using PU film as the dielectric layer.

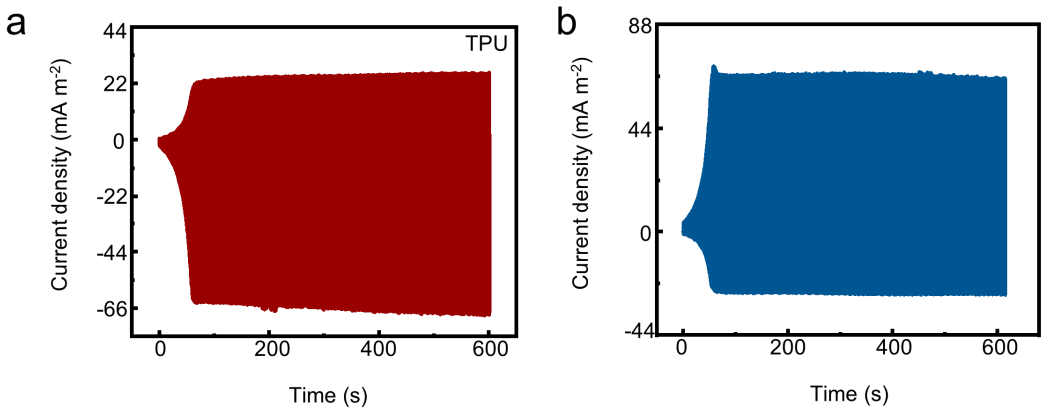

Fig. S31: The output characteristics of UH-CSI-TENG with TPU as triboelectric material. a) Dynamic current density output with positive charge injection, and b) Dynamic current density output with negative charge injection, using TPU film as the dielectric layer.

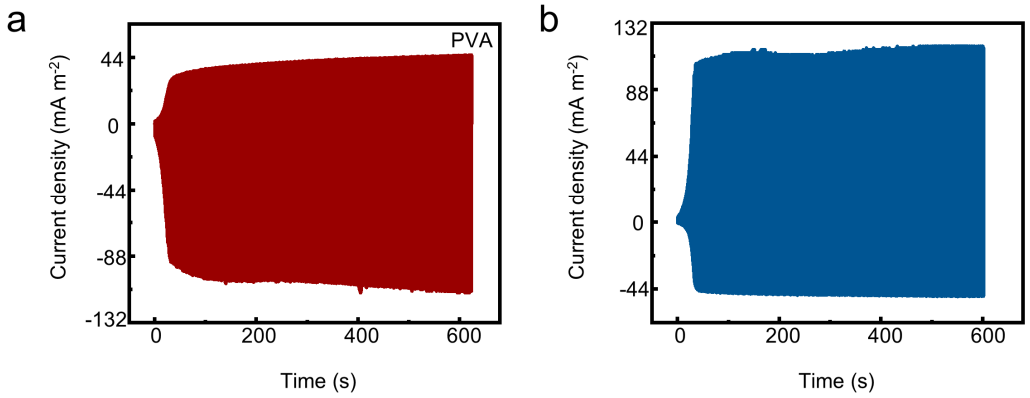

Fig. S32: The output characteristics of UH-CSI-TENG with PVA as triboelectric material. a) Dynamic current density output with positive charge injection, and b) Dynamic current density output with negative charge injection, using PVA film as the dielectric layer.

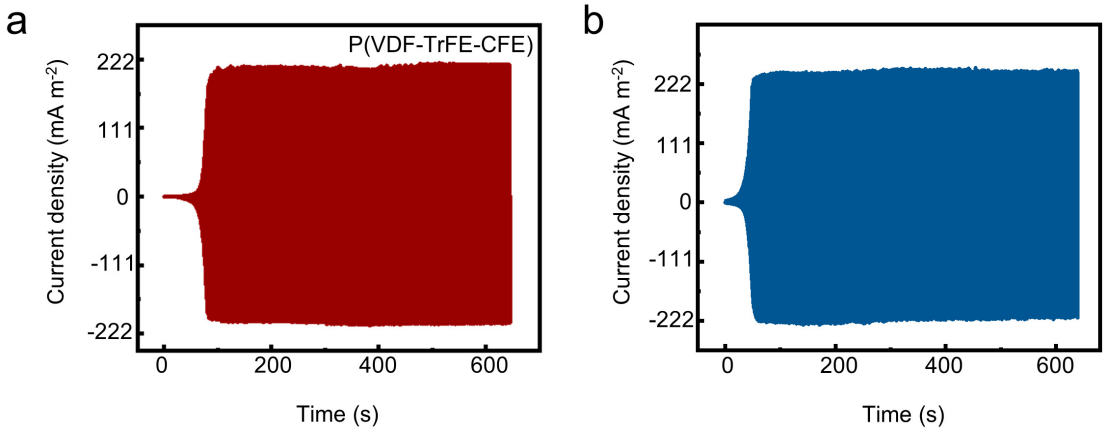

Fig. S33: The output characteristics of UH-CSI-TENG with P(VDF-TrFE-CFE) as triboelectric material. a) Dynamic current density output with positive charge injection, and b) Dynamic

current density output with negative charge injection, using P(VDF-TrFE-CFE) film as the dielectric layer.

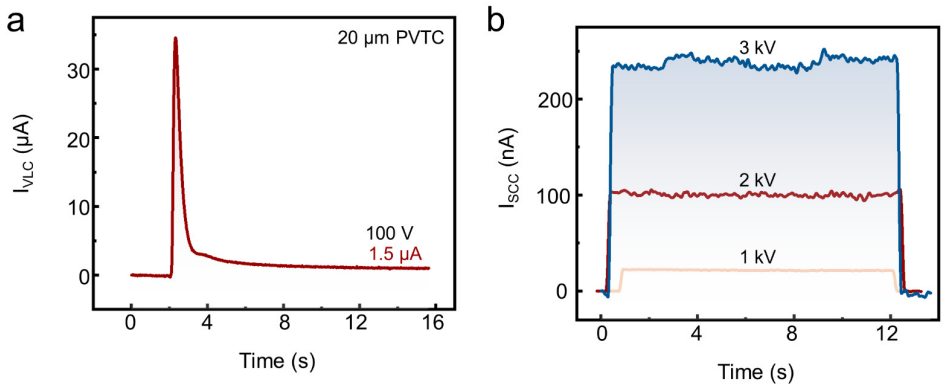

Fig. S34: Charge leakage current and surface conduction current of PVTC. a) Charge leakage current at a voltage of 100V. b) Surface conduction current at different voltages.

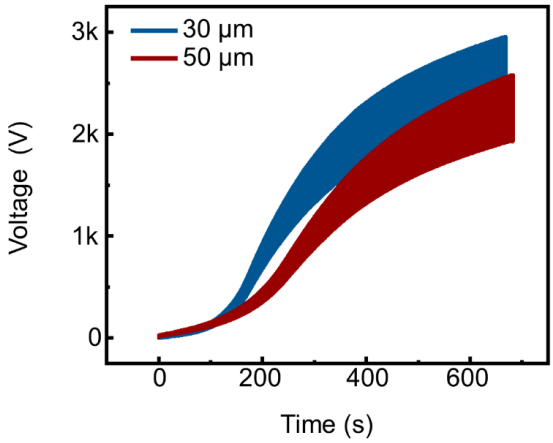

Fig. S35: Dynamic excitation voltage of PI with different thickness.

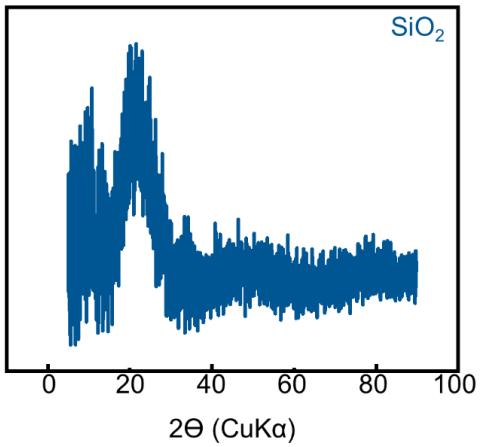

Fig. S36: Crystalline phase of silica.

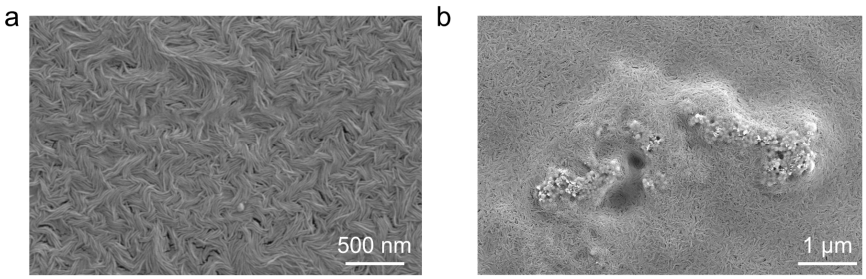

Fig. S37: SEM image of charge transport layer. a) Normal doping. b) Excessive doping.

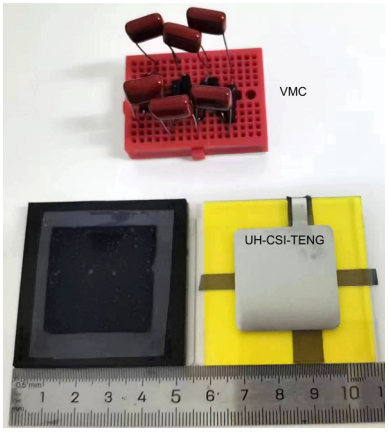

Fig. S38: Structure configuration of UH-CSI-TENG.

Table S1. Output charge density and charge dissipation rate comparison in the developmental stage of TENG

Materials	Charge density ($\mu C\ m^{-2}$)	Charge dissipation rate	Modification method	Years	Literature
PET&KH556	77.6	86%	Deep Trap Construction	2024	Adv. Mater. 2024, 2303389
Mxene/TiO_2	128	58.3%	Electron trapping & blocking effect	2022	Nano Energy 98 (2022) 107236
PTFE	190	10%	Surface-charge engineering	2021	J. Mater. Chem. A, 2021, 9, 21357–21365
ECTFE	391	48%	Quenching polarization	2023	Adv. Funct. Mater. 2023, 33, 2302164
FEP	510	-	Repeated rheological forging	2022	NATURE COMMUNICATIONS | (2022) 13:4083
Ionized-PTFE	525	-	Radical anion transfer	2023	Matter 6, 1295–1311
PI	880	45%	External charge excitation	2022	Adv. Funct. Mater. 2022, 32, 2203884

MoS_2/SiO_2	1072	25%	Electric-field-driven interfacial trapping of drifting	2023	Energy Environ. Sci., 2023, 16, 598–609
PI	1480	64.4%	Discharge Mitigation Strategy	2023	Adv. Energy Mater. 2023, 13, 2302099
P(VDF-TrFE)	2670	92%	Ultra-Fast Charge Self-Injection Technique	2024	Adv. Mater. 2024, 2312148
This work	3880	40%	Optimize trap distribution and construct charge transfer/blocking layer	2024	

Table S2. Quantify the charge (positive/negative) trapping and de-trapping ability of traditional triboelectric materials

Materials	Full name	Positive charge (nC)	Positive charge dissipation rate	Negative charge (nC)	Positive charge dissipation rate
ETFE	Ethylene-terafluoroethlene	240	41.6%	280	42.8%
PCTFE	Polychlorotrifluroethylene	265	16.9%	300	0.07%
FEP	Fluorinated ethylene propylene	270	11.1%	300	0.01%
BOPP	Biaxially oriented polypropylene	260	0.01%	310	0.01%
PTFE	Polytetrafluoroethylene	290	0.03%	310	0.01%
POF	Polyolefin	400	31.2%	385	23.3%
PP	Polypropylene	450	22.2%	490	15.3%
PFA	Perfluoroalkoxy	410	24.3%	500	14%
PVC	Polyvinyl chloride	700	34.3%	670	0.08%
PI	Polyimide	690	10.1%	830	9.63%
PVDC	Polyvinylidene chloride	1150	89.5%	1150	86.1%
P(VDF-HFP)	Poly(vinylidene fluoride-co-hexafluoropropylene)	1200	96.7%	1300	95.3%
PVDF	Polyvinylidene fluoride	1200	88.3%	1320	65.2%
P(VDF-TrFE)	Poly (vinylidene fluoride-trifluoroethylene)	1700	90.1%	1800	84.4%
PPS	Polyphenylene sulfide	235	0.06%	240	16.7%
PS	Polystyrene	265	50.9%	240	62.5%
PE	Polyethylene	345	63.7%	320	81.2%

PDMS	Polydimethylsiloxane	350	8.5%	350	11.4%
PMMA	Polymethyl Methacrylate	390	48.7%	355	69.1%
PEEK	Poly(ether-ether-ketone)	420	0.1%	400	12.5%
PC	Polycarbonate	550	0.03%	510	15.7%
PAN	Polyacrylonitrile	670	67.1%	700	74.3%
PA	Polyamide	700	25.7%	700	40%
PET	Polyethylene terephthalate	760	0.05%	720	11.1%
PLA	Polylactic acid	800	92.5%	800	92.5%
PEI	Polyetherimide	1400	32.1%	1500	45.3%

Note S1: Calculate the trap state distribution of dielectric polymer

The details of calculation are based on the theory proposed by Simmons and Tam, it is assumed that the trapping process does not occur after the charge is trapped during the surface potential decay process, and the composite behavior of holes and electrons is ignored. The current density J formed by the holes excited to the valence band can be expressed as:

$$J = \frac{qL}{2}\int_{E_V}^{E_F}\left(1 - f_0(E)\right) N_t(E) e_n(E) e^{-e_n t} dE \quad (1)$$

where q is the hole charge amount; L is the thickness of the sample; E is the energy level; E_F is the Fermi level; E_V is the highest energy level in the valence band; $f_0(E)$ is the initial electron occupancy of the trap; $N_t(E)$ is the continuous distribution function of traps; define a local state hole trap in the forbidden band as E_m, then the probability $e_n(E)$ of the hole trap excited by $E = E_m – E_V$ on the valence band is

$$e_n(E) = ve^{-\frac{E}{k_B T}} = ve^{-\frac{E_m - E_v}{k_B T}} \quad (2)$$

where v is the escape frequency factor of the trap charge; k_B is the Boltzmann constant; T is the absolute temperature. The function $G(E, t)$ is introduced as

$$G(E,t) = e_n e^{-e_n t} = B\delta(E - E_m) \quad (3)$$

where $G(E, t)$ represents the weight of the trap electron with energy level E at the time t to the discharge current; $\delta(E–Em)$ is the impulse function. Integrate both sides of eq 3, B is given by

$$B = \int_{E_V}^{E_F} e_n(E) e^{-e_n(E)t} dE = \frac{k_B}{t}(1 - e^{-vt}) \approx \frac{k_B}{t} \quad (4)$$

Substituting eq 4 into eq 1, and setting $f_0(E) = 0.5$, J is given by

$$J = \frac{qLk_B T}{4t} N_t(E) \quad (5)$$

Meanwhile, the current density J can be expressed as the surface potential decay process as

$$J = \frac{\varepsilon_0 \varepsilon_r}{L}\left|\frac{dV_S(t)}{dt}\right| \quad (6)$$

where ε_0 is the dielectric constant of the vacuum; ε_r is the relative dielectric constant of the sample; $V_s(t)$ is the surface potential value of the sample at time t. Simultaneously eqs 5 and 6, $Nt(E)$ is given by

$$N_t(E) = \frac{4\varepsilon_0 \varepsilon_r}{qL^2 T K_B}\left|t\frac{dv_{S(t)}}{dt}\right| \quad (7)$$

Trap energy E can be expressed as

$$E = E_m - E_V = k_B T \ln(vt) \quad (8)$$

and the surface potential decay curve is fitted to obtain the $V_s(t)$ function expression. Using the eqs 7 and 8, the trap energy of the sample can be obtained distribution characteristics. Experiments show that the ISPD curve of dielectric layers can be well fitted by using the double exponential function. The expression of the double exponential function is

$$V_S(t) = A_1 e^{-t/\tau_1} + A_2 e^{-t/\tau_2} \quad (9)$$

where *A1*, *A2* and τ_1, τ_2 are fitting parameters. Use eqs 7 and 8 to calculate the trap level distributions corresponding to the two parts $A_1 e^{-t/\tau_1}$ and $A_2 e^{-t/\tau_2}$, and obtain the energy level distribution characteristics corresponding to the two trap centers.

*k_B=1.38×$10^{23}$$m^2$$kg^{s-2}$$K^{-1}$; *v*= 4.1×$10^{13}$$s^{-1}$; ε_0=8.85×10^{-12} F/m; *T*=298.15K; *q*=1.602×10^{-19}C.

Note S2: Measure charge leakage current and surface conduction current

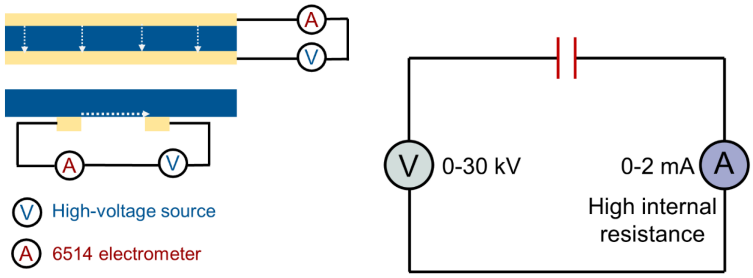

1) A copper metal layer of about 1μm is hot evaporated onto the sample's surface to assemble a capacitor. The current passing through the capacitor is recorded using an electrometer.

2) It is worth noting that the leakage current (I_{VLC}) of the polymer consists of the conductive leakage current (I_L), capacitive charge leakage current (I_C), and polarization absorption leakage current (I_A). Here, I_L characterizes the insulation ability of the polymer and needs to be read after the current maintains stability.

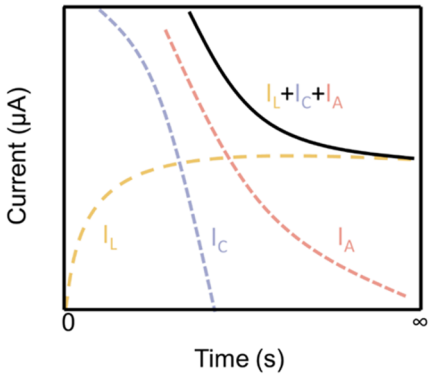

Conductive leakage current (I_L) is a small amount of current (usually measured in microamperes) that flows through insulation, between conductors, or from conductors to the ground. Since it is relatively stable and time-independent, this is the most crucial current to measure insulation resistance. Capacitive charge leakage current (I_C) is caused by the capacitance effect, when a DC voltage is applied, this current lasts only a few seconds and gradually decreases until the capacitor is fully charged. Polarization absorption leakage current (I_A) is caused by molecular polarization within dielectric materials. In low-capacitance devices, the current is high for the first few seconds and slowly decreases to almost zero.

3) I_{SCC} is determined only by the surface conductance of the dielectric polymer, independent of polarization absorption leakage current and capacitive charge leakage current.

Note S3: Surface potential measurement by KPFM

Tips of KPFM measurements (Dimension icon, Bruker) coated Pt/Ir layer with a typical tip radius of ~ 20 nm, resonant frequency of ~ 75 kHz and force constant k of ~ 2.8 N/M. The lift height of tip is set to 50 nm and employing the tapping mode is used. The spatial resolution of KPFM is about in the order of several tens of nanometers.

The experiment begins in contact mode with an applied voltage of 2V. The scanning area of the polymer is 2x2 μm, and the scanning frequency is 0.1 Hz. After that, it switches to non-contact mode with a fixed needle tip 50 nm away from the polymer. The surface potential of the polymer is scanned in real time, and then the potential is scanned again one hour later.

There are many influence factors that could influence our KPFM tests such as probe tip condition, surface adsorption or doping, probe lift height, probe biased voltage, surrounding environment, etc. To make sure the accuracy of KPFM, all the tests are on the same tip for a specific sample to minimize the tip effect.